

GRAPHENE ANTENNA DESIGN AND CHARACTERISATION FOR FIFTH  
GENERATION APPLICATIONS

SITI NOR HAFIZAH BINTI SA'DON

A thesis submitted in fulfilment of the  
requirements for the award of the degree of  
Doctor of Philosophy

School of Electrical Engineering  
Faculty of Engineering  
Universiti Teknologi Malaysia

MAY 2020

## **DEDICATION**

I dedicate this thesis to all my family members

Especially my parents, Mr. Sa'don and Mrs. Sarah, my husband, Mr. Aniq, my son,  
Firas and my siblings, you all are my inspiration

I could not accomplished this doctoral journey without your prayer, support,  
understanding and contribution of time, May Allah Bless all of you

Thank you, Allah for giving me the strength to continue on this challenging journey

## ACKNOWLEDGEMENT

From the starting of this research work until preparing this thesis, I was in contact with many people, researchers, academicians, and practitioners. They have contributed towards my understanding and thoughts. In the beginning, I wish to express my sincere appreciation to my main supervisor, Associate Professor Dr. Mohd Haizal bin Jamaluddin, for valuable advice and support this research. He has delivered very well guidance, finance, discussions, and constructive critics throughout this research until finding the results. Then, I would like to acknowledge my external supervisor, who is my former main supervisor, Associate Professor Dr. Muhammad Ramlee bin Kamarudin, who guide and give me a chance in the title's selection for my doctorate study. His support, finance, encouragement, knowledge, motivation and comment are very helpful. He also has struggled in searching and contacting with persons who work in graphene field. I am also very thankful to my co-supervisor Dr. Fauzan bin Ahmad for the knowledge and support in the part of graphene and facilities. Without his precious support and interest, this graphene research work could not be continued.

I am also indebted to Kementerian Pengajian Tinggi Malaysia for funding my Ph.D study through MyBrain15-MyPhD. Then, Perpustakaan Sultanah Zanariah at Universiti Teknologi Malaysia also deserve special thanks for their assistance in supplying the relevant literatures especially through e-journal.

My sincere appreciation also extends to all my colleagues for their views and tips which are useful indeed, and thanks for the fun-time together. Not forget to the fellow friends and staffs at Wireless Communication Centre, Material Science Laboratory and Malaysia-Japan International Institute of Technology at Universiti Teknologi Malaysia, and Institut Teknologi Maju at Universiti Putra Malaysia who gave me access to the laboratory and research facilities, besides provided assistance at various occasions.

Last but not the least, I would like to thank my family: my parents, my husband, my son and my siblings for supporting me spiritually throughout this study and my life.

## ABSTRACT

The incoming fifth generation (5G) technology requires antennas with a greater capacity, wider wireless spectrum utilisation, high gain, and beam steering ability. This is due to the cramped spectrum utilisation in the previous generation. As a matter of fact, conventional antennas are unable to serve the new frequency due to the limitations in fabrication and installation mainly for smaller sizes. The use of graphene material promises antennas with smaller sizes and thinner dimensions, yet capable of emitting higher frequencies. Graphene is a unique material that can display tuning characteristics. This characteristic originates from its surface complex conductivity, which is controlled by a chemical potential. Most characteristics of tunable graphene antenna have been studied on terahertz frequency range, thus making it difficult to be realised practically. Besides, the standard antenna that uses switching components may have trouble during installation, and size consuming as it can be seen in the reconfigurable antenna. Due to that, another study to produce graphene with excellent properties is vital for the advancement of wireless communication system. In this thesis, graphene antennas for fifth generation applications are conducted in three parts of studies. In the first part, the graphene antenna properties are studied in different curing temperatures and times. The curing temperatures are 250°C, 300°C, and 350°C, then each temperature is set with curing times of 20 minutes, 30 minutes, 1 hour, 2 hours, and 3 hours to manufacture graphene based antenna with different properties. The proposed graphene based antenna properties are then respectively investigated using performance network analyser (PNA), vector network analyser (VNA), field-emission scanning electron microscope (FESEM), and Raman spectroscopy. From analyses on the dielectric, conductivity and characterisation on graphene's physique, the antenna properties exhibit a tunability through its resonance frequency and main beam direction of the radiation pattern by the variation obtained in curing temperature and time. In the same time, the gain of the antennas can also be varied. The second part is the study of graphene antennas at a frequency of 15 GHz in both single and array elements. The high-frequency antenna contributes to a large bandwidth and is excited by coplanar waveguide for easy fabrication on one surface via screen printing method. The defected ground structure is applied in an array element to improve the radiation and increase the gain. The results show that the printed graphene antenna for single element produces an impedance bandwidth, gain, and efficiency of 48.63%, 2.99 dBi, and 67.44%, respectively. Meanwhile, the array element produces slightly better efficiency (72.98%), approximately the same impedance bandwidth as the single element (48.98%), but higher gain (8.41 dBi). Moreover, it provides a beam width of 21.2° with scanning beam capability from 0° up to 39.05°. The last part is a tunable antenna based on graphene operating at microwave frequency range is proposed. The antenna is designed and fabricated at 15 GHz with a gate electrode placed behind it. They are connected to external direct current (DC) bias during the measurement. The biasing is applied from 0 V to 30 V. The result shows that the resonance frequency is tuned to 20 MHz and reflection coefficient magnitude improves by 1.24 dB. Following this, an analytical calculation on chemical potential is also derived to enhance the graphene tunability. It is shown that at least 2.85 kV of the gate voltage is needed to vary the chemical potential and less than 0.29  $\mu\text{m}$  of dielectric thickness is suitable for tuning purpose with a given condition. Based on the three parts of studies on antenna design and characterisation, graphene can be a good alternative material for future communication. It is due to the exhibited performances are comparable with conventional material and could act beyond the common antenna properties under the influence of tunability, which is owned by graphene.

## ABSTRAK

Teknologi generasi kelima (5G) yang akan datang memerlukan antena dengan lebih kapasiti, penggunaan spektrum tanpa wayar yang lebih luas, gandaan yang tinggi, dan kebolehan pengemudian alur. Ini disebabkan oleh penggunaan spektrum yang sempit pada generasi terdahulu. Sebagai hakikatnya, antena konvensional tidak mampu untuk menyediakan frekuensi baru disebabkan oleh batasan fabrikasi dan pemasangan terutamanya untuk saiz yang lebih kecil. Penggunaan bahan graphene menjanjikan antena dengan ukuran yang lebih kecil dan dimensi yang lebih nipis, namun mampu memancarkan frekuensi yang lebih tinggi. Graphene adalah satu bahan unik yang boleh memaparkan ciri penalaan. Ciri ini berasal dari kekonduksian kompleks permukaannya, yang dikawal oleh potensi kimia. Kebanyakan ciri antena graphene boleh tala telah dikaji pada julat frekuensi terahertz, oleh itu menjadikannya sukar untuk direalisasikan secara praktikal. Di samping itu, antena piawai yang menggunakan komponen pensuisan mungkin mengalami masalah semasa pemasangan, dan mengambil saiz seperti yang boleh dilihat dalam antena boleh konfigurasi semula. Oleh sebab itu, satu lagi kajian untuk menghasilkan graphene dengan sifat yang sangat baik adalah penting untuk kemajuan sistem komunikasi tanpa wayar. Dalam tesis ini, antena graphene untuk aplikasi generasi kelima dikendalikan kepada tiga bahagian kajian. Pada bahagian pertama, sifat antena graphene dikaji pada suhu dan masa pengawetan berbeza. Suhu pengawetan adalah 250°C, 300°C, dan 350°C, kemudian setiap suhu ditetapkan dengan masa pengawetan selama 20 minit, 30 minit, 1 jam, 2 jam, dan 3 jam untuk menghasilkan antena berasaskan graphene dengan ciri yang berbeza. Ciri antena berasaskan graphene yang dicadangkan kemudiannya masing-masing disiasat menggunakan penganalisis rangkaian prestasi (PNA), penganalisis rangkaian vektor (VNA), mikroskop elektron pengimbasan pemancaran medan (FESEM), dan spektroskopi Raman. Dari analisis dielektrik, kekonduksian dan pencirian pada sifat graphene, sifat antena menunjukkan keupayaan boleh tala melalui frekuensi resonans dan arah alur utama pola sinaran dengan perubahan yang diperolehi di dalam suhu dan masa pengawetan. Pada masa yang sama, gandaan antena juga boleh diubah. Bahagian kedua ialah kajian terhadap antena graphene pada frekuensi 15 GHz dalam kedua-dua elemen tunggal dan tatasusunan. Antena frekuensi tinggi menyumbang kepada lebar jalur yang besar dan diuja oleh pandu gelombang sesatah untuk lebih memudahkan fabrikasi pada satu permukaan melalui teknik percetakan skrin. Struktur pembumian cacat digunakan dalam elemen tatasusunan untuk memperbaiki radiasi dan meningkatkan gandaan. Keputusan menunjukkan bahawa antena graphene yang dicetak untuk elemen tunggal menghasilkan lebar jalur galangan, gandaan, dan kecekapan masing-masing sebanyak 48.63%, 2.99 dBi dan 67.44%. Sementara itu, elemen tatasusunan menghasilkan kecekapan yang sedikit lebih baik (72.98%), kira-kira lebar jalur galangan yang sama seperti elemen tunggal (48.98%), tetapi gandaan yang lebih tinggi (8.41 dBi). Selain itu, ia memberikan lebar alur 21.2° dengan kemampuan pengimbasan alur dari 0° sehingga 39.05°. Bahagian terakhir ialah antena boleh tala berasaskan graphene beroperasi pada julat frekuensi gelombang mikro dicadangkan. Antena direka bentuk dan difabrikasi pada 15 GHz dengan elektrod get yang diletakkan di belakangnya. Ia disambungkan pada pincangan arus terus (DC) luaran semasa pengukuran. Pincangan digunakan dari 0 V hingga 30 V. Hasilnya menunjukkan bahawa frekuensi resonans ditala kira-kira 20 MHz dan magnitud pekali pantulan meningkat 1.24 dB. Berikutan itu, pengiraan analisis ke atas potensi kimia juga diterbitkan untuk meningkatkan keupayaan boleh tala graphene. Ia menunjukkan bahawa sekurang-kurangnya 2.85 kV voltan get diperlukan untuk mengubah potensi kimia dan kurang daripada 0.29 μm ketebalan dielektrik adalah sesuai untuk tujuan penalaan dengan keadaan tertentu. Berdasarkan ketiga-tiga bahagian kajian ke atas reka bentuk dan pencirian, graphene boleh menjadi bahan alternatif yang baik untuk komunikasi masa hadapan. Ini kerana, prestasi yang ditunjukkan adalah sebanding dengan bahan konvensional dan boleh bertindak melangkaui ciri antenna biasa di bawah pengaruh kebolehan boleh tala yang dimiliki oleh graphene.

## TABLE OF CONTENTS

	<b>TITLE</b>	<b>PAGE</b>
	<b>DECLARATION</b>	<b>iii</b>
	<b>DEDICATION</b>	<b>iv</b>
	<b>ACKNOWLEDGEMENT</b>	<b>v</b>
	<b>ABSTRACT</b>	<b>vi</b>
	<b>ABSTRAK</b>	<b>vii</b>
	<b>TABLE OF CONTENTS</b>	<b>viii</b>
	<b>LIST OF TABLES</b>	<b>xii</b>
	<b>LIST OF FIGURES</b>	<b>xiv</b>
	<b>LIST OF ABBREVIATIONS</b>	<b>xxiii</b>
	<b>LIST OF SYMBOLS</b>	<b>xxvii</b>
	<b>LIST OF APPENDICES</b>	<b>xxxii</b>
<b>CHAPTER 1</b>	<b>INTRODUCTION</b>	<b>1</b>
1.1	Introduction	1
1.2	Problem Statement	3
1.3	Objectives	7
1.4	Scopes	7
1.5	Thesis Organisation	8
<b>CHAPTER 2</b>	<b>LITERATURE REVIEW</b>	<b>11</b>
2.1	Introduction	11
2.2	Fifth Generation	11
2.2.1	Definition and Requirements	12
2.3	Fifth Generation Antenna and Properties	13
2.3.1	Bandwidth Improvement	13
2.3.2	Gain Enhancement	18
2.3.3	Mutual Coupling Reduction	26
2.3.4	Beam Scanning	31

2.3.5	Evaluation on the Previous Works	34
2.4	Graphene	41
2.4.1	Definition and Structure	41
2.4.2	Electronic Properties	42
2.4.3	Tunable Characteristics	43
2.4.3.1	Electric Field Doping or DC Bias	44
2.4.3.2	Chemical Doping, Structural Modifications or Defects	45
2.4.4	Graphene Surface Complex Conductivity	45
2.4.5	Opportunity of Graphene in 5G Antenna Applications	47
2.5	Graphene Antenna	48
2.5.1	Graphene Patch Antenna	49
2.5.2	Tunable Graphene Antenna	57
2.5.3	Evaluation on the Previous Works	61
2.6	Graphene Affected by Temperature	65
2.6.1	Relation of Curing Temperature in Microwave Absorption and Electrical Properties of Graphene	65
2.6.2	The Previous Work on Graphene Affected by Temperature	67
2.7	Summary	75
<b>CHAPTER 3</b>	<b>RESEARCH METHODOLOGY</b>	<b>77</b>
3.1	Introduction	77
3.2	Antenna Specification	77
3.2.1	Graphene Dispersion with Ethyl Cellulose in Terpinol	79
3.2.2	Conductive Graphene Sheet	79
3.2.3	Flexible Kapton® Type HN Polyimide Film	80
3.3	Flow Chart	81
3.4	Research Methodology	87
3.5	Antenna Design and Estimation	88
3.6	Simulation Tools	91
3.7	Fabrication Process	91

3.7.1	Screen Printing Method	91
3.7.2	Electronic Cutting Tool Method	94
3.8	Measurement Process	96
3.8.1	S-parameter Measurement	96
3.8.2	Radiation Pattern Measurement and Gain Calculation	98
3.8.3	Dielectric and Conductivity Measurement	101
3.8.4	Surface Morphology Characterisation	103
3.8.5	Structure Analysis	103
3.9	Summary	104
<b>CHAPTER 4</b>	<b>ANALYSIS OF GRAPHENE ANTENNA PROPERTIES FOR 5G APPLICATIONS</b>	<b>105</b>
4.1	Introduction	105
4.2	Single Element Graphene Antenna	106
4.2.1	Design Evolutions	106
4.2.2	Parametric Studies	107
4.2.3	Properties of Graphene Based Antenna Affected by Curing Temperature and Time	109
4.2.3.1	Microwave Absorption / Antenna Properties	109
4.2.3.2	Electrical Properties	115
4.2.3.3	Physical Properties	120
4.2.4	CPW-fed Chamfer-shaped with Rectangular Slot Antenna Based on Graphene	125
4.2.5	Results	127
4.3	Antenna Array	130
4.3.1	Mutual Coupling Reduction	131
4.3.2	Inter-Element Spacing	134
4.3.3	Results	136
4.3.4	Scanning Performance	140
4.4	Summary	141



<b>CHAPTER 5</b>	<b>CHARACTERISATION OF TUNABLE GRAPHENE ANTENNA</b>	<b>143</b>
5.1	Introduction	143
5.2	Tunable Antenna Design Based on Graphene	141
5.2.1	Antenna Design	144
5.2.2	Parametric Study	146
5.3	Result and Analysis	147
5.3.1	Measurement Results	148
5.3.2	Experiment Using External DC Bias	152
5.3.3	Analytical Calculations	153
5.4	Summary	156
<b>CHAPTER 6</b>	<b>CONCLUSION AND FUTURE WORKS</b>	<b>157</b>
6.1	Conclusion	157
6.2	Future Works	158
<b>REFERENCES</b>		<b>159</b>
<b>LIST OF PUBLICATIONS</b>		<b>175</b>
<b>APPENDICES</b>		<b>177</b>

## LIST OF TABLES

<b>TABLE NO.</b>	<b>TITLE</b>	<b>PAGE</b>
Table 2.1	The previous works on bandwidth improvement in 5G	36
Table 2.2	The previous works on gain enhancement in 5G	37
Table 2.3	The previous works on mutual coupling reduction in 5G	39
Table 2.4	The previous works on beam steering in 5G	40
Table 2.5	The previous works on graphene patch antenna	62
Table 2.6	The previous works on tunable graphene antenna	64
Table 3.1	The design specification and properties of graphene antenna in different part of studies	78
Table 4.1	Data of resonance frequency after curing temperature and time	111
Table 4.2	Main lobe direction of the radiation pattern and calculated antenna gain with variation of curing times and temperatures	114
Table 4.3	Dielectric constant and dielectric loss determination on graphene antenna after curing time and temperature	117
Table 4.4	Conductivity measurement and reference of sheet resistance after curing process	119
Table 4.5	Summary of intensity and ratio	125
Table 4.6	Summary of printed graphene antenna parameter, description, and length	127
Table 4.7	Detail of printed graphene antenna properties for simulation and measurement	130
Table 4.8	Specifications of printed graphene antenna array before introducing the rectangular slot and after introducing the rectangular slot	134
Table 4.9	Detail of simulation and measurement of antenna array performance	139
Table 4.10	Simulated beam steering performance	140
Table 5.1	Summarisation of antenna parameters	147

Table 5.2	The comparison of antenna characteristics without gate electrode and with the gate electrode	151
Table 5.3	The listed tuning effect during the biasing application	153
Table 5.4	The calculation of gate voltage and dielectric spacer thickness based on specified condition above	155

## LIST OF FIGURES

FIGURE NO.	TITLE	PAGE
Figure 1.1	The service provided by 1G to 4G is limited for people whereas 5G covers people and things [18]	2
Figure 2.1	5G provides massive performances to support the multiple connections [63]	12
Figure 2.2	The broadband antenna for 5G from (a) Top view (b) Bottom view [66]	15
Figure 2.3	The measured and simulated reflection coefficient magnitude together with simulated realised gain at the top side of the graph [66]	15
Figure 2.4	The printed antenna made by silver and MDC that display front view (left) and back view (right) [67]	16
Figure 2.5	(a) The comparison of simulated and measured reflection coefficient magnitude (b) The measured antenna efficiency and realised gain [67]	16
Figure 2.6	(a) The fabricated flexible antenna (b) The simulated and measured of reflection coefficient magnitude [68]	17
Figure 2.7	(a) The circle shows microstrip-to-slot-line and rectangular slot at at top layer and bottom layer of dipole antenna (b) The simulated and measured reflection coefficient magnitude and gain [69]	17
Figure 2.8	The printed elliptical slot/monopole antenna with (a) sector-disc radiating patch from the top view (b) rectangular slot in the ground plane from the bottom view [66]	19
Figure 2.9	(a) The simulated gain from CST and HFSS at 28 GHz and 38 GHz (b) Measured radiation pattern at E-plane (top) and H-plane (bottom) [66]	20
Figure 2.10	(a) The slot aperture at ground plane without RDR (b) The ground plane mounted with RDR at $TE_{181}^y$ (c) The ground plane mounted with RDR at $TE_{183}^y$ [71]	20
Figure 2.11	The radiation pattern at (a) E-plane (b) H-plane [71]	21
Figure 2.12	The arrow marks parasitic cell on PLDPA	21

Figure 2.13	The results of (a) Measured gain and reflection coefficient magnitude (b) The measured radiation pattern at E-plane (top) and H-plane (bottom) [72]	22
Figure 2.14	(a) The AVA array design with labelled MDs and CGEs (b) The measured radiation pattern at E-plane (left) and H-plane (right) [73]	22-23
Figure 2.15	(a) The location of U-shaped lens on 1 x 4 antenna array (b) The increment of gain by using U-shaped lens [74]	23
Figure 2.16	The design of CPW fed rectangular patch array antenna [75]	24
Figure 2.17	The simulated and measured of (a) Reflection coefficient magnitude (b) Gain and efficiency (c) Radiation pattern at H-plane (left) and E-plane (right) for frequency of 36 GHz [75]	24
Figure 2.18	The antenna array from back view (top) and front view (bottom) [76]	25
Figure 2.19	The result of simulated and measured (a) Reflection coefficient magnitude (b) Antenna gain and efficiency, and (c) Radiation pattern at several planes [76]	25
Figure 2.20	(a) Stub is located in between two dipoles at ground plane (b) 8-element array antenna [69]	26
Figure 2.21	(a) Simulated mutual coupling for two dipoles antenna in the variation of stub length (b) Simulated and measured radiation pattern for 28 GHz at E-plane and H-plane [69]	27
Figure 2.22	The back view and front view of AVA array (left) side and AVA-CR array (right) [77]	27
Figure 2.23	The comparison of AVA array and AVA-CR array in (a) Isolation (b) Gain (c) Radiation pattern at both E-plane and H-plane for 26 GHz (top), and 28 GHz (bottom) [77]	28
Figure 2.24	(a) The circled on T-junction marked as Taylor distribution (b) The fabricated SIW array antenna with several layer of substrates [80]	29
Figure 2.25	(a) Simulated reduced mutual coupling and gain (b) Radiation pattern at x-z plane (top) and y-z plane (bottom) [80]	29
Figure 2.26	The antenna without EBG as reference (left) and proposed antenna with EBG (right) [81]	30
Figure 2.27	The comparison results of (a) S21 (b) Radiation pattern at YOZ and XOY plane [81]	30

Figure 2.28	(a) The two antennas design for notch (left) and aperture-coupled (right) (b) The location of antenna array at mobile terminal [82]	31
Figure 2.29	The total scan pattern for both types of antenna array [82]	32
Figure 2.30	The antenna configuration [83]	32
Figure 2.31	The pattern of measured beam scanning [83]	32
Figure 2.32	The quad-mode planar antenna in (a) Mobile terminal simulation design (b) Fabrication [84]	33
Figure 2.33	The measured beam scanning of quad-mode planar array [84]	33
Figure 2.34	(a) The design of cavity-backed slot antenna array (b) The fabricated antenna at mobile device casing [85]	34
Figure 2.35	The measured beam scanning [85]	34
Figure 2.36	Graphene in a form of (a) carbon bonds [91] and (b) like-honeycomb lattice [92]	42
Figure 2.37	The structures of $sp^2$ carbon are found in (a) Graphite (3D) (b) Graphene (2D) (c) Carbon nanotube (1D) and (d) Fullerene (0D) [90]	42
Figure 2.38	The zero bandgap at Dirac point also located at $K'$ point in hexagonal structure of graphene [96]	43
Figure 2.39	The trend of (a) conductivity [87] and (b) sheet resistivity [90] in gate voltage variation	44
Figure 2.40	The graphene conductivity in the function of frequency	46
Figure 2.41	The trend of conductivity for intra band in chemical potential range [95], whilst inter-band in the graph can be ignored since it is not involved in this study	47
Figure 2.42	The fabricated graphene meandered-line antenna [122]	49
Figure 2.43	The simulated and measured (a) Reflection coefficient magnitude at several case (b) Gain at the range of 835 MHz to 900 MHz (c) Radiation pattern at E-plane (left) and H-plane (right) [122]	49-50
Figure 2.44	(a) The fabricated graphene-based dipole antenna and measured (b) Reflection coefficient magnitude (c) Gain and efficiency (c) Radiation pattern [123]	50-51
Figure 2.45	The front view (left) and back view (right) of dual band graphene antenna [125]	51

Figure 2.46	The comparison of simulated and measured S11 [125]	51
Figure 2.47	(a) The fabricated graphene elliptical antenna (b) The comparison of reflection coefficient magnitude [126]	52
Figure 2.48	The simulated and measured (a) Radiation pattern at $\phi = 0^\circ$ (left) and $\phi = 90^\circ$ (right) (b) Gain and directivity (c) Antenna efficiency. ORT is optical-to-RF transformer. [126]	52-53
Figure 2.49	a) The fabricated CPW fed slot antenna (b) Measured reflection coefficient magnitude and gain (c) Measured radiation pattern. The labelled (a)-(d) means unbended and bended with radius 5.0 cm, 3.5 cm, and 2.5 cm, respectively [128]	53-54
Figure 2.50	(a) The fabricated rectangular microstrip patch antenna (b) Measured reflection coefficient magnitude and (c) Measured radiation pattern at E-plane (left) and H-plane (right) for FGF and copper [137]	54-55
Figure 2.51	The monopole antenna made by graphene mixed polyaniline [139]	55
Figure 2.52	The measured return loss for (a) 2D and (b) 3D monopole antenna [139]	55
Figure 2.53	The measured directivity, gain, and radiation efficiency [139]	56
Figure 2.54	(a) The graphene microstrip antenna array and comparison result of (b) S-parameters (c) Measured radiation pattern for each port and (d) Gain [140]	56
Figure 2.55	The structure of hybrid graphene-metal at THz band [106]	57
Figure 2.56	The measured (a) Tunable resonance frequency and (b) Radiation pattern at $\mu_c = 0.5$ eV [106]	57-58
Figure 2.57	(a) The antenna structure (b) Measured tunable reflection coefficient magnitude (c) Measured radiation pattern at 10 GHz [51]	58-59
Figure 2.58	The tunable S11 in two DC voltage values [52]	59
Figure 2.59	(a) The small graphene patch is marked by arrow (b) The tuning frequency in the range of 0 V to -20 V [141]	60
Figure 2.60	The fabricated tunable planar antenna with deposited FLG [142]	61
Figure 2.61	(a) Measured tunable resonance frequency (b) The reading of tunable resonance frequency and measured gain [142]	61

Figure 2.62	(a) The SEM image and (b) The conductivity with line marked '1', '2', and '3' for nanocomposite with GNPs of 0.32 wt%, 6.4 wt%, and 9.6 wt%, respectively [148]	68
Figure 2.63	(a) The SEM image of graphene (b) Reflection loss occurred in composite with 7 wt% of graphene (c) The reflection loss and frequency tuning at different temperature in composite with 7 wt% of graphene (d) The trend of imaginary permittivity of composite in different weight percentage of graphene [57]	69
Figure 2.64	The SEM surface image for (a) 1300°C (b) 1500°C and (c) 1700°C [149]	70
Figure 2.65	The Raman Spectrum analysis (b) The ratio obtained from the Raman Spectrum [149]	70
Figure 2.66	The SEM image at (a) 850°C (b) 900°C, and (c) 950°C [150]	71
Figure 2.67	The SEM image for Ti composite reinforced with RGO at (a) 800°C (b) 900°C (c) 1000°C and (d) 1100°C	72
Figure 2.68	The Raman spectrum	72
Figure 2.69	(a) The Raman spectra of graphene/Cu at several annealing temperature (b) The sheet resistance in increasing temperature for IGZO/Ti/graphene/PI [152]	73
Figure 2.70	(a) The dielectric constant and dielectric loss in temperature variation (b) The reflection loss in the change of temperature [59]	74
Figure 2.71	(a) The real and imaginary permittivity in temperature variation (b) The shifted reflection loss and resonance frequency in temperature variation [58]	74
Figure 3.1	The graphene is packed in 10 mL in glass bottle	79
Figure 3.2	The graphene sheet [156]	80
Figure 3.3	The Kapton film can be laminated, metallised, punched, formed or adhesive coated [157]	80
Figure 3.4	The procedure of designing graphene antennas for 5G applications	81-86
Figure 3.5	The tools in the fabrication of screen printing	92
Figure 3.6	(a) The arrangement of equipment while screen printing (b) The deposited ink on stencil (c) The best incline position of squeegee rubber is at 45° (d) The graphene ink is printed on Kapton polyimide film substrate	93



Figure 3.7	(a) The furnace displays timing of treatment while curing the graphene ink (b) The black colour of graphene ink before curing process turned grey colour after the treatment	94
Figure 3.8	The materials utilised in cutting tool	95
Figure 3.9	(a) The graphene sheet is placed between transparent film and A4 paper (b) The pattern of antenna formed after cutting	95
Figure 3.10	(a) The Kapton film before cutting and (b) The Kapton film after cutting	96
Figure 3.11	The interface of performance network analyser	97
Figure 3.12	(a) Calibration kit : Open, Short, Load (b) The selection of calibration kits : 85056D, DUT Connectors : APC 2.4 male, Port 1 (c) Calibration : Open (d) Calibration : Short (e) Calibration : Load (f) After calibration is done	97-98
Figure 3.13	The horn antenna as transmitter and AUT as receiver while the PC and PNA are the part of control system	99
Figure 3.14	The received power is recorded on (a) test antenna, and (b) standard antenna	100
Figure 3.15	The dielectric and conductivity measurement requires VNA, personal computer with DAK Software, and probe	101
Figure 3.16	The graphene antenna is inserted in probe to measure dielectric and conductivity	102
Figure 3.17	The FESEM is connected to PC for collecting the image characterised [164]	103
Figure 3.18	The Raman spectroscopy [165]	104
Figure 4.1	The evolution of proposed printed graphene antenna with CPW-fed (a) rectangular shaped, (b) semi-rectangular slot, (c) rectangular slot, (d) rectangular slot with chamfer	106
Figure 4.2	The resonance frequency is tuned by modification of the CPW ground	107
Figure 4.3	The response of the reflection coefficient and resonance frequency on the (a) dielectric constant of the substrate, (b) the conductivity of graphene, and (c) the length of cut	108
Figure 4.4	The measured reflection coefficient shows resonance frequency tuned after antenna is applied with different curing temperatures of (a) 250°C (b) 300°C (c) 350°C and time	110

Figure 4.5	Graph of resonance frequency versus curing temperature at different curing times	112
Figure 4.6	Beamforming of radiation pattern observable at E-plane while remain unchanged at H-Plane with rise of curing temperature and time	112-113
Figure 4.7	(a) Main lobe direction tuned from a negative direction to a positive direction (b) The increment of gain calculated	115
Figure 4.8	Graphs of (a) dielectric constant and (b) dielectric loss with variation of curing time and temperature	118
Figure 4.9	Conductivity of graphene antenna is proportional to the curing temperature and time	119
Figure 4.10	FESEM images of graphene antenna is prepared in different curing time and temperatures (a) 20 minutes (250°C) (b) 30 minutes (250°C) (c) 1 hour (250°C) (d) 2 hours (250°C) (e) 3 hours (250°C) (f) 20 minutes (300°C) (g) 20 minutes (350°C), respectively	120-121
Figure 4.11	Raman spectrum of graphene antenna	122
Figure 4.12	Raman spectrum of graphene antenna at (a) G peak (b) D peak and (c) 2D peak	123-124
Figure 4.13	(a) Parameter of printed graphene antenna with CPW-fed rectangular slot with chamfer, (b) The printed graphene antenna is assembled with SMA connector	126
Figure 4.14	Simulation and measurement of reflection coefficient magnitude, represented by a solid curve and dashed curve, respectively	128
Figure 4.15	Comparison of simulated and measured radiation patterns at (a) E-plane and (b) H-plane	129
Figure 4.16	The radiation pattern measurement is read together with the (a) L-shaped adaptor and (b) the SMA connector	129
Figure 4.17	Printed graphene antenna array, (a) before introducing rectangular slot, (b) after introducing the rectangular slot	131
Figure 4.18	Isolation of printed graphene antenna array, (a) before rectangular slot, (b) after rectangular slot	132
Figure 4.19	Radiation patterns of printed graphene antenna array before introducing rectangular slot and after introducing the rectangular slot, at (a) E-plane and (b) H-plane	132
Figure 4.20	Current distribution (a) before introducing rectangular slot, (b) after introducing the rectangular slot	133
Figure 4.21	Trend of gain value in the range of inter-element spacing	135

Figure 4.22	Isolation of $S_{12}$ parameter at 15 GHz in variation of inter-element spacing	135
Figure 4.23	Fabricated 4-element printed graphene antenna array, (a) with SMA connector, (b) connected to <i>Re-Formable Semi-Rigid Cable Assemblies</i> and external 1-to-4 power divider	136
Figure 4.24	Reflection coefficient magnitude of the antenna array, showing simulated $S_{11}$ in a solid curve and measured $S_{11}$ in a dashed curve	137
Figure 4.25	S-parameter of printed graphene antenna array for, (a) simulation, (b) measurement	137
Figure 4.26	Comparison result for radiation pattern of printed graphene antenna array at, (a) E-plane, and (b) H-plane	138
Figure 4.27	The radiation pattern measurement read together with (a) re-formable semi-rigid cable assemblies and (b) the holder and tape to attach on the foam	139
Figure 4.28	Simulation of beam scanning array	140
Figure 5.1	(a) Antenna design with parameter from the top view represented by grey colour which is graphene sheet while yellow colour at the bottom layer is Kapton film, (b) The fabricated antenna from graphene sheet is connected to SMA connector	144
Figure 5.2	Gate electrode is located at the back side of tunable antenna (a) The layer in part of gate electrode (b) Graphene patch and copper are connected to external DC bias and SMA connector is connected to PNA	145
Figure 5.3	Schematic diagram for connection between tunable graphene antenna, external DC bias and PNA	146
Figure 5.4	The simulation result of reflection coefficient magnitude in the changing of graphene sheet resistance	147
Figure 5.5	The reflection coefficient magnitude for simulation and measurement without gate electrode and with the gate electrode	148
Figure 5.6	The simulation and measurement of radiation pattern at: (a) E-plane; (b) H-plane without a gate electrode; and (c) E-plane (d) H-plane with the gate electrode	150
Figure 5.7	The directive main beam shows beamwidth at -3 dB without gate electrode and with gate electrode, respectively	151

Figure 5.8	The experiment of tunable graphene antenna through PNA while performing the biasing application	152
Figure 5.9	The tunable effect when DC bias is applied from 0 V to 30	153

## LIST OF ABBREVIATIONS

1G	-	First Generation
SMS	-	Short Message Service
2G	-	Second Generation
3G	-	Third Generation
4G	-	Fourth Generation
LTE-A	-	Long Term Evolution-Advanced
5G	-	Fifth Generation
IoT	-	Internet of Thing
M2M	-	Machine-to-Machine
Gbps	-	Gigabits per second
GHz	-	Gigahertz
mm-Wave	-	Millimeter-Wave
WRC	-	World Radio Conference
IMT	-	International Mobile Telecommunications
dBi	-	Decibels Relative to Isotropic
mm	-	millimeter
SLL	-	Side Lobe Level
PCBs	-	Printed Circuit Boards
RFIC	-	Radio Frequency Integrated Circuit
DC	-	Direct Current
THz	-	Terahertz
CPW	-	Coplanar Waveguide
DGS	-	Defected Ground Structure
Mbps	-	Megabits per second
ms	-	milliseconds
Tbps	-	Terabits per second
MMC	-	Massive Machine Communication
$Mn_{0.2}Zn_{0.8}Fe_2O_4$	-	Manganese Zinc Ferrite
MDC	-	Microwave Dielectric Ceramic
MPA	-	Microstrip Patch Antenna

PET	-	Polyethylene Terephthalate
RDR	-	Rectangular Dielectric Resonator
PLDPA	-	Printed Log-Periodic Dipole Array
CGEs	-	Gradual Corrugated Edges
MDs	-	Metal Directors
AVA	-	Antipodal Vivaldi Antenna
3D	-	Three-Dimensional
dB	-	Decibels
SIC	-	Substrate Integrated Cavity
HPBW	-	Half-Power Beamwidth
CR	-	Coupling Reduce
SIW	-	Substrate Integrated Waveguide
EBG	-	Electronic Band Gap
FR-4	-	Flame Retardant-4
AoA	-	Angle of Arrival
UWB	-	Ultra-Wideband
CNT	-	Carbon Nanotube
2D	-	Two-dimensional
0D	-	Zero-dimensional
1D	-	One-dimensional
3D	-	Three-dimensional
m/s	-	meter per second
$\text{cm}^2\text{V}^{-1}\text{s}^{-1}$	-	square centimeter per Volt per second
RF	-	Radio Frequency
SEM	-	Scanning Electron Microscopy
TEM	-	Transmission Electron Microscopy
AFM	-	Atomic Force Microscopy
S	-	Siemens
SI	-	International System of Units
S/m	-	Siemens per meter
eV	-	electron Volt
K	-	Kelvin
ps	-	picosecond

V	-	Volt
RFID	-	Radio-Frequency Identification
MHz	-	Megahertz
$\Omega$ /sq	-	Ohm per square
FGF	-	Flexible Multi-Layer Graphene Film
PANI	-	Polyaniline
ISM	-	Industrial, Scientific, And Medical
SiO <sub>2</sub>	-	Silica / Silicon Dioxide
Si	-	Silicon
Ag	-	Silver
CVD	-	Chemical Vapor Deposition
GSG	-	Ground-Signal-Ground
VNA	-	Vector Network Analyser
MST	-	Modulated Scattering Technique
FLG	-	Few-Layer Graphene
CF	-	Carbon Fiber
wt%	-	Weight percentage
GNPs	-	Graphene Nanoplatelets
PS	-	Polystyrene
GO	-	Graphene Oxide
GF	-	Graphene Film
I <sub>D</sub> /I <sub>G</sub>	-	The Ratio Between Intensity of D and G Band
RGO	-	Reduced Graphene Oxide
Ti	-	Titanium
Cu	-	Copper
PI	-	Polyimide
IGZO	-	Indium Gallium Zinc Oxide
MWNT	-	Multiwalled CNT
$\Omega$ .cm	-	Ohm centimeter
nm	-	nanometer
$\mu$ m	-	micrometer
kHz	-	kilohertz
CST	-	Computer Simulation Technology

PNA	-	Performance Network Analyser
FESEM	-	Field-Emission Scanning Electron Microscope
CPU	-	Central Processing Unit
RAM	-	Random Access Memory
PC	-	Personal Computer
SMA	-	Sub Miniature Version A
AUT	-	Antenna Under the Test
EBSD	-	Electron Backscatter Diffraction
kV	-	kilovolt
STEM	-	Scanning Transmission Electron Microscopy
TEM mode	-	Transverse Electromagnetic mode
MIC	-	Microwave Integrated Circuit
MMIC	-	Monolithic Microwave Integrated Circuit
PVAL	-	Polyvinyl Alcohol
MV	-	Medium Voltage
cm	-	centimeter



## LIST OF SYMBOLS

$\%$	-	Percentage
$R_{max}$	-	Maximum Data Rate
$B$	-	Bandwidth
$M$	-	The Discrete Levels of Signals
$S$	-	Signal Power
$N$	-	Noise Power
$E$	-	Total Field
$AF$	-	Array Factor
$n$	-	The Number of Elements
$\theta_o$	-	Angle Observed
$d$	-	Separation Between Elements / Inter-element Spacing
$\beta$	-	Progressive Phase Shift
$P_r$	-	The Power Delivered to the Receiving Antenna / Received Power of Test Antenna
$P_t$	-	The Input Power of the Transmitting Antenna
$R$	-	The Distance Between Two Antennas
$G_T$	-	The Gain of Transmitting Antenna / Gain of AUT
$G_R$	-	The Gain of Receiving Antenna
$D$	-	The Largest Dimension of Antenna
$\lambda$	-	The Wavelength
$TE_{1\delta 3}^y$	-	Higher Order Mode
$TE_{1\delta 1}^y$	-	Fundamental Mode
$\delta$		The Fraction of Half-Cycle of the field variation
$^\circ$	-	Degree
$v_F$	-	Fermi Velocity
$\sigma$	-	Conductivity
$V_g$	-	Gate Voltage
$\rho$	-	Sheet Resistivity / Bulk Resistivity
$n$	-	Surface Charge Density

$\epsilon_0$	-	Dielectric Permittivity of Free Space
$\epsilon_r$	-	Dielectric Constant of Substrate / Relative Complex Permittivity
$t_s$	-	Substrate Thickness
$e$	-	Electron Charge
$\omega$	-	Angular Frequency
$\mu_c$	-	Chemical Potential
$T$	-	Temperature
$\Gamma$	-	Scattering Rate
$\tau$	-	Transport Relaxation Time
$k_B$	-	Boltzmann Constant
$\hbar$	-	Reduced Plank's Constant
$\pi$	-	pi
$\pm$	-	Plus-minus
$^{\circ}C$	-	Degree Celcius
$\Omega$	-	Ohm
$mL$	-	Milliliter
$P_S$	-	Received Power of Standard Antenna
$G_S$	-	Gain of Standard Antenna
$e_o$	-	Total Antenna Efficiency
$e_r$	-	Reflection (mismatch) Efficiency
$e_{cd}$	-	Antenna Radiation Efficiency
$\Gamma_{RL}$	-	Voltage Reflection Coefficient
$\epsilon'$	-	Real Part of Permittivity / Dielectric Constant
$\epsilon''$	-	Imaginary Part of Permittivity / Dielectric Loss
$\tan(\delta)$	-	Loss Tangent
$W_p$	-	Patch Width
$c$	-	Velocity of Light
$f_o$	-	Center Frequency
$L_p$	-	Patch Length
$L_{eff}$	-	Effective Length
$\Delta L$	-	Length Extension

$\epsilon_{eff}$	-	Effective Dielectric Constant
$D_{cpw}$	-	Distance of Separation Between the Two Ground Planes of Waveguide
$s1$	-	Slot Width Between Ground Plane and Feedline
$W_f$	-	Feedline Width / Center Strip Conductor Width
$Z_o$	-	Characteristic Impedance
$W_s$	-	Substrate Width
$L_s$	-	Substrate Length
$\theta_c$	-	Angle of Chamfer Structure
$L_f$	-	Feedline Length
$W_g$	-	Ground Plane Width Between Slot and Feedline
$L_g$	-	CPW Length
$s2$	-	Side Slot
$s3$	-	Top Slot
$t_g$	-	Graphene Thickness
$L_c$	-	Length of Cut
$W_d$	-	Slot Width
$L_d$	-	Slot Length
$S_{11}$	-	Reflection Coefficient Magnitude
$\epsilon_s$	-	Static Permittivity
$\epsilon_\infty$	-	Relative Dielectric Permittivity
$\tau(T)$	-	Temperature Relaxation Time
$E_a$	-	Activation Energy
$\tau_o$	-	Prefactor
$R_c$	-	Gas Constant
$\sigma(T)$	-	Temperature-Dependent Electrical Conductivity
$RL$	-	Return Loss
$Z_{in}$	-	Normalised Input Impedance
$f$	-	Microwave Frequency
$\mu_r$	-	Relative Permeability
$R_o$	-	Resistance
$R_s$	-	Sheet Resistance

- $t$  - The Thickness of Resistor
- $l$  - The Length of Resistor
- $w$  - The Width of Resistor

## LIST OF APPENDICES

<b>APPENDIX</b>	<b>TITLE</b>	<b>PAGE</b>
Appendix A	MATLAB Code for Calculating Graphene Conductivity	177
Appendix B	Data Sheet and Product Specification of Graphene Dispersion With Ethyl Cellulose In Terpeneol	178
Appendix C	Data Sheet of Conductive Graphene Sheet	188
Appendix D	Technical Data Sheet of Flexible Kapton® type HN Polyimide Film	195
Appendix E	Data Sheet of Horn Antenna (Standard Antenna) Gain	199
Appendix F	MathLAB Code for Calculating Minimum Gate Voltage	206
Appendix G	MathLAB Code for Calculating Minimum Gate Voltage from Other References	207
Appendix H	MathLAB Code for Calculating Maximum Dielectric Thickness	208
Appendix I	MathLAB Code for Calculating Maximum Dielectric Thickness from Other References	209

# CHAPTER 1

## INTRODUCTION

### 1.1 Introduction

Wireless communication technology evolves in every ten years. The evolution occurs to serve the improvement service for current requirement so that interaction between people can be implemented properly from time to time. Historically, wireless communication technology has started in 1981 with analogue system. At the moment, the phone only limited for voice communication [1] and this era is known as the first generation (1G). Then in 1992, a digital system was introduced where users can start employ short message service (SMS) text messaging [2]. The existed system is categorised as second generation (2G). Next, in year 2001, the third generation (3G) has started by expanding digital technology through multimedia transmission [3] in mobile phone, laptop and computers. The multimedia consists of high-speed internet access, highly-improved video and audio streaming capabilities [1]. While in 2011 until recent, fourth generation (4G) has taken place to provide high bandwidth access and it is recognised as Long Term Evolution-Advanced (LTE-A) [1], [4]. The 4G LTE technology has become the world information, social media and news can be reached instantly, able facilitating our daily work and life [5] likes online shopping, learning, meeting or even handling business, home work, leisure, and transportation [6] with just in our fingertips by simply using smart phones.

In the coming of 2020 and beyond, the researchers and scientists anticipate that fifth generation (5G) comes with greater capacity and implement new spectrum [7]. The 5G is depicted that it will involve new complementary technologies such as machine-type communication or known as Internet of Thing (IoT), beamforming, front and backhaul, hot spots and small cells [8]. As reported in [9], it states that 5G will support stringent latency, reliability, wide range of data rates, and network scalability and flexibility. Thus, there are a huge number of antenna devices will be installed in

the extending of 5G technology [10] likes on-body [11], building or any constructions [6], electrical appliances [12], and private or public transport [13]. Based on these scenarios, the 5G antenna in mobile terminal should have good properties for supporting this new features such as high gain [14], antenna array [15], multiple antenna [16], switched antenna [16], beam-forming [17], and high-directivity beam steering [12]. Figure 1.1 shows the communication evolution from 1G to 5G.

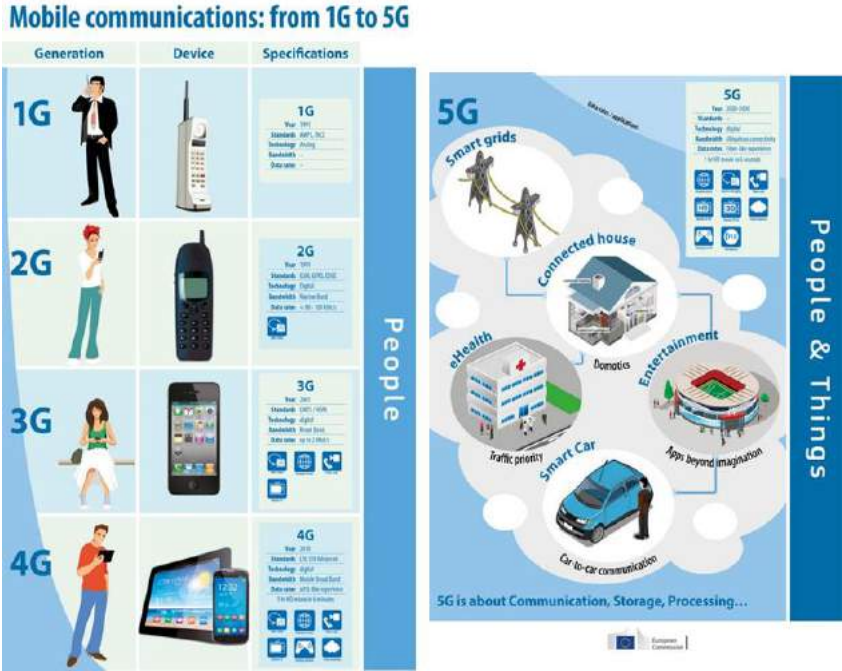


Figure 1.1 The service provided by 1G to 4G is limited for people whereas 5G covers people and things [18]

Therefore, in the 5G antenna design, it is not enough to utilise conventional materials at all kind of 5G applications. It is because some applications appropriate to certain materials in order to keep the aesthetic value, comfortability, and quality. These scenarios become a big challenge in the antenna design. Accordingly, it is time for researchers and scientists in the antenna field to make a paradigm shift. The antenna design is not just made by common conductive and substrate, but can be developed from others potential materials which benefits in the antenna performance as will be introduced in this work that is graphene.

## 1.2 Problem Statement

With the development of wireless communication technology towards 5G by 2020, the total of device will become larger and could hit up to ten or hundreds billions [4]. This fact is supported by [19] where the huge number is came from machine-to-machine (M2M) applications. That means, the mobile phone that subscribes mobile broadband every year can reach more than one hundred fold. The rise number of machine as a result of people desire the Internet access for immediate communication and access information [10]. Hence, this situation bring to a limit which make the current communication unable to support the mobile data traffic.

The first problem is identified that the [12] predicted the data traffic will go beyond 17 exabytes ( $17 \times 10^{18}$  bytes) per month with combining mobile phones, laptops, tablets, and M2M. While in [7] mentioned that the heavy data is coming from video where mobile users start watching television programs and movies through streaming video. Due to that, the mobile traffic will reach 291.8 exabytes in a year by 2019 [7], [20]. The forecast will become worst as the available frequency spectrum allocated, that is lower than 3 GHz has been fully utilised [19]. The same limitation was also presented in [21] where the frequency below 6 GHz is extremely crowded with mobile systems, broadcasting and satellite. This situation brings the spectrum enter the maximum usage [11] thus make the lower frequency unable to serve high bandwidth anymore [10], [14].

Based on this limitation, the demand on higher capacity can be solved by providing broad range of frequency or large bandwidth in order to provide high data rate service [21]. The data rate must exceed 1 Gbps [1], [8], [11], [12] and could reach 50 Gbps [22] which means the possible bandwidth is 1 GHz [7], [12], [22]. Due to cramped utilisation at low frequency, a new frequency spectrum need to be explored and proposed for the future communication. It is supported by [22] where the greater bandwidth can be obtained at higher frequency which able to support higher speed. Several high frequencies have been proposed. Samsung's technology has designed frequency near to millimeter wave (mm-Wave) which range from 30 GHz to 300 GHz [11]. Whilst the other researchers has proposed several tens of gigahertz (GHz), such



as 28 GHz and 38 GHz [1], [12], [23], [24], free licensed of 60 GHz [14], and E band; 71 GHz to 76 GHz, 81 GHz to 86 GHz and 92 GHz to 95 GHz [7], [12], [15], [25]. Besides that, the World Radio Conference, Geneva in 2019 (WRC 19) has regulated that 24.5 GHz to 86 GHz can be used for future development of International Mobile Telecommunication (IMT) [26]. Since all the spectrum is not defined yet, thus the frequency that can be considered is band above 6 GHz as stated in the Office of Communications (Ofcom), United Kingdom [22]. However, this work considers frequency in between 6 GHz to 20 GHz because it is not explored as much as mm-Wave, while equipment and facilities in this frequency can be obtained easily.

The second problem is, the conventional indoor antenna commonly has omnidirectional radiation in between -8 dBi to 0 dBi [14]. The gain is too low in order to support the forthcoming 5G system which involves an indoor communication within 80 % compared to outdoor in about 20 % [10], [25], [27]. While that, mm-Wave will experience some disturbances compared to lower frequency because, the signal becomes weak during penetration on solid material or building wall [1], absorbed or scattered by gases, rain, foliage [11], and flora [27]. The path loss also will affect the data rate, spectral efficiency, and energy [10]. In conjunction, the lower frequency band resulting larger antenna size, if the antenna array is designed at this frequency for solving the interference or increasing gain. The antenna will be bulky and not practical for current devices. Furthermore, a very high frequency will face a challenge in manufacturing antenna [8] since the antenna size is inversely proportional to the operating frequency. Due to that, a conventional material and fabrication method used in common antenna also has limitation to manufacture a smaller antenna size which has gap of 0.1 mm.

Related to the problem above, the indoor communication requires higher penetration of radiation. A signal can penetrate with higher gain by implementing antenna array [11] and considering the beam steering and narrow beam [14]. Thus, the gain should be achieved by mobile terminal is near to 12 dBi [28]. In the antenna array design, the isolation for each S-parameter between antenna elements and radiation pattern must be obtained properly in order to obtain high gain. Thus, a technique of mutual coupling reduction can be implemented to reduce side lobe level (SLL) and

improve gain. In the production of antenna either single element or array, this study will integrate with alternative materials, graphene as conducting element. It is due to the difference application commonly requires particular material mainly to save cost, besides being flexible, easy, fast, suitable for small size production, and lightweight. Some devices may even be down-scaled [29] in size because of the higher frequency spectrum utilisation. Thus graphene is one of the alternative selection since it has an advantage to produce small dimension which means can be fabricated from nanometers to centimeters [30], [31], and promising candidates to decrease the antenna size [32]. In addition, graphene also can produce broad bandwidth to solve the first problem aforementioned.

The third problem is spotted on multifunctional and multipurpose devices in future communication. The feature is important since the current environment forces people to perform many types of communication and execute many tasks simultaneously involving an antenna which is adaptive with any situation or frequency needed. Due to that, a combination antenna from several frequencies will enlarge the antenna size. In addition, the thickness of cellular phone printed circuit boards (PCBs) are not more than 1 mm thus any increase in the PCB thickness is directly related to rise the production costs and size of the design in the fiercely competitive consumer electronics arena [14]. The difficulties may occurred because the communication device, installation and maintenance should be cheap and reduce cost [12].

Accordingly, a tunable antenna is suitable because its performance is the same as that of a multiple antenna. Since it can cover multiple operating frequencies, then it tends to reduce the system size and number of components [33] besides to serve the device into compact size [34], additional functionalities and attractive features [35], respectively. Tunable antennas commonly implement switches [33], [36]–[43] for varying operating frequency. However, the switches installation possibly disrupt the antenna performance. The other method that presents the same effect employs the implementation of certain materials, where they can be in the form of substrate, radiating or receiving element or additional antenna layer [34], [35], [44], [45]. Thus it is appropriate to envisage the radio frequency integrated circuit (RFIC) with material likes silicon, semiconductors or any material embedded [14], [46]–[48] by a direct

current (DC) biasing exhibit switching characteristics. It is applicable because graphene also has tunable properties [49]. This effect is caused by its surface complex conductivity, which is controlled via chemical doping by changing the gate voltage applied [49], [50].

However, several problems are pointed out on graphene where it exhibits big shifted resonance frequency during measurement, broad bandwidth, and unstable radiation pattern due to losses on graphene conductivity and uncontrolled graphene properties that are obtained after curing process. Then, a small changes of resonance frequency and return loss at microwave range [51], [52] are exhibited if tunability is studied. Applying a high voltage to tune the resonance frequency or using a tiny substrate based on the surface charge density equation [53] can solve the limitation, theoretically. Different responses at frequency range near to 1 terahertz (THz) [54] indicate a definite change of tuning due to the high dependence on chemical potential at THz range [55], which means the conductivity of graphene varies smoothly when a chemical potential is changed. Thus, nano-size antenna should be produced for obtaining THz range but it only can be achieved with the support of adequate facilities.

With these deficiencies, there is an alternative method to investigate the characteristics of graphene and at the same time to study the tunability of graphene antenna that is through the disturbance by external energy, or temperature exposure. Since graphene that used in this study have to go through curing process, so it is suitable to use temperature as the factor of change. Temperature also is one of the variable which can modify the conductivity of graphene besides using chemical potential [56]. With the effect of temperature on graphene, the carbon structure of graphene can be changed then affected the electrical properties which directly tune the antenna properties likes resonance frequency [57], [58], reflection coefficient magnitude [59], and radiation pattern if it is in a form of antenna. This mechanism can be an alternative way to be integrated in communication device for future technology.

### **1.3 Objectives**

The objectives of the research are :

- (a) To investigate the characteristics of graphene antenna in term of electrical and physical properties
- (b) To design, fabricate and test the performance of graphene antenna for single and array element to achieve 5G antenna requirement
- (c) To analyse the tunable properties of graphene antenna

### **1.4 Scopes**

The scopes of the research are :

- (a) The graphene antenna is investigated in a range of temperature and time exposed. The investigation covers the same fifteen single antennas that classified into three curing temperature; 250°C, 300°C and 350°C. Each curing temperature has the curing time at 20 minutes, 30 minutes, 1 hour, 2 hours and 3 hours. The antenna properties are studied in the variation of curing temperature and time. The change of relative complex permittivity and structure of graphene are recorded for supporting the study.
- (b) The single element and phased array of graphene antenna are studied at frequency of 15 GHz using of coplanar waveguide (CPW). The requirement for 5G antenna covers resonance frequency, reflection coefficient magnitude, bandwidth, percentage of impedance bandwidth, radiation pattern, gain and total efficiency. The array antenna studies are limited to four elements due to availability of a four port-external power divider. The defected ground

structure (DGS) is implemented as the mutual coupling reduction and beam steering ability is examined in simulation only.

- (c) Tunable antenna is analysed using a single element. The antenna operates at the same frequency of 15 GHz. A gate electrode is placed at the back side of antenna for biasing purpose. The biasing analysed covers from 0 V to 30 V and the tunable properties is observed at the resonance frequency and reflection coefficient magnitude. Then, an analytic calculation is suggested for the possibility value for tuning to be happened.

## **1.5 Thesis Organisation**

This thesis is distributed into seven chapters. Chapter 1 has introduced the background and evolution of 5G, the problem and proposed solution for antenna in 5G including the objectives and scopes of the thesis. Chapter 2 presents the literature review of 5G and graphene. The 5G covers definition, requirement and 5G antenna properties such as bandwidth improvement, gain enhancement, mutual coupling reduction, and beam scanning which are reviewed from the previous study. The graphene part touches graphene definition, graphene structure, electronic properties, tunable characteristics, graphene surface conductivity, and opportunity of graphene in 5G applications. The graphene antenna which is graphene patch antenna, and tunable graphene antenna are reviewed from the previous work. The relation of graphene between temperature and microwave absorption is carried out together with previous study on graphene affected by temperature.

Chapter 3 explains the methodology of this research. This chapter contains the antenna specification, flow chart, research methodology, antenna design and estimation, simulation tools, fabrication process, and measurement process. Chapter 4 discusses the properties of 5G antenna made by graphene in single and array element. This chapter contains antenna design and estimation, design evolution, parametric studies, investigation of graphene antenna properties in a range of curing temperature

and time with the justification of dielectric, conductivity, surface morphology, and carbon structure, and measurement result for single element. While array element analyses mutual coupling reduction, inter-element spacing, measurement results, and beam scanning performance.

Next, in Chapter 5, the study presents tunable graphene antenna using DC voltage. Then a calculation is derived to analyse the possible value that can show tunability using provided antenna specification. Finally, Chapter 6 concludes the findings of all this research, highlights the contribution, and recommendation for future work.

## REFERENCES

- [1] T. S. Rappaport *et al.*, “Millimeter Wave Mobile Communications for 5G Cellular: It Will Work!,” *IEEE Access*, vol. 1, pp. 335–349, 2013.
- [2] G. Wunder *et al.*, “5GNOW: Non-orthogonal, asynchronous waveforms for future mobile applications,” *IEEE Commun. Mag.*, vol. 52, no. 2, pp. 97–105, Feb. 2014.
- [3] Z. Ying, “Antennas in cellular phones for mobile communications,” *Proc. IEEE*, vol. 100, no. 7, pp. 2286–2296, Jul. 2012.
- [4] J. G. Andrews *et al.*, “What Will 5G Be?,” *IEEE J. Sel. Areas Commun.*, vol. 32, no. 6, pp. 1065–1082, Jun. 2014.
- [5] G. Liu, Y. Huang, F. Wang, J. Liu, and Q. Wang, “5G features from operation perspective and fundamental performance validation by field trial,” *China Commun.*, vol. 15, no. 11, pp. 33–50, Nov. 2018.
- [6] C.-L. I, S. Han, Z. Xu, S. Wang, Q. Sun, and Y. Chen, “New Paradigm of 5G Wireless Internet,” *IEEE J. Sel. Areas Commun.*, vol. 34, no. 3, pp. 474–482, Mar. 2016.
- [7] M. Shafi *et al.*, “5G: A Tutorial Overview of Standards, Trials, Challenges, Deployment, and Practice,” *IEEE J. Sel. Areas Commun.*, vol. 35, no. 6, pp. 1201–1221, Jun. 2017.
- [8] S. Mattisson, “An Overview of 5G Requirements and Future Wireless Networks: Accommodating Scaling Technology,” *IEEE Solid-State Circuits Mag.*, vol. 10, no. 3, pp. 54–60, 2018.
- [9] A. Osseiran *et al.*, “Scenarios for 5G mobile and wireless communications: The vision of the METIS project,” *IEEE Commun. Mag.*, vol. 52, no. 5, pp. 26–35, May 2014.
- [10] C. X. Wang *et al.*, “Cellular architecture and key technologies for 5G wireless communication networks,” *IEEE Commun. Mag.*, vol. 52, no. 2, pp. 122–130, Feb. 2014.
- [11] A. Bleicher, “The 5G phone future [News],” *IEEE Spectr.*, vol. 50, no. 7, pp. 15–16, Jul. 2013.

- [12] C. Dehos, J. González, A. Domenico, D. Kténas, and L. Dussopt, “Millimeter-wave access and backhauling: The solution to the exponential data traffic increase in 5G mobile communications systems?,” *IEEE Commun. Mag.*, vol. 52, no. 9, pp. 88–95, Sep. 2014.
- [13] H. Ullah, N. Gopalakrishnan Nair, A. Moore, C. Nugent, P. Muschamp, and M. Cuevas, “5G Communication: An Overview of Vehicle-to-Everything, Drones, and Healthcare Use-Cases,” *IEEE Access*, vol. 7, pp. 37251–37268, 2019.
- [14] Wonbin Hong, Kwang-Hyun Baek, Youngju Lee, Yoongeon Kim, and Seung-Tae Ko, “Study and prototyping of practically large-scale mmWave antenna systems for 5G cellular devices,” *IEEE Commun. Mag.*, vol. 52, no. 9, pp. 63–69, Sep. 2014.
- [15] F. Boccardi, R. Heath, A. Lozano, T. L. Marzetta, and P. Popovski, “Five disruptive technology directions for 5G,” *IEEE Commun. Mag.*, vol. 52, no. 2, pp. 74–80, Feb. 2014.
- [16] D. Muirhead, M. A. Imran, and K. Arshad, “A Survey of the Challenges, Opportunities and Use of Multiple Antennas in Current and Future 5G Small Cell Base Stations,” *IEEE Access*, vol. 4, pp. 2952–2964, 2016.
- [17] Dinh-Thuy Phan-Huy, M. Sternad, and T. Svensson, “Making 5G Adaptive Antennas Work for Very Fast Moving Vehicles,” *IEEE Intell. Transp. Syst. Mag.*, vol. 7, no. 2, pp. 71–84, 2015.
- [18] G. Champeau, “5G, or its usefulness according to the European Commission,” 2014. [Online]. Available: <https://www.numerama.com/magazine/28542-5g-internet-objets-reseau-europe.html>. [Accessed: 14-Nov-2019].
- [19] S. Chen and J. Zhao, “The requirements, challenges, and technologies for 5G of terrestrial mobile telecommunication,” *IEEE Commun. Mag.*, vol. 52, no. 5, pp. 36–43, May 2014.
- [20] T. S. Rappaport, G. R. MacCartney, M. K. Samimi, and S. Sun, “Wideband Millimeter-Wave Propagation Measurements and Channel Models for Future Wireless Communication System Design,” *IEEE Trans. Commun.*, vol. 63, no. 9, pp. 3029–3056, Sep. 2015.
- [21] B. Bangerter, S. Talwar, R. Arefi, and K. Stewart, “Networks and devices for the 5G era,” *IEEE Commun. Mag.*, vol. 52, no. 2, pp. 90–96, Feb. 2014.



- [22] O. UK, "Spectrum above 6 GHz for future mobile communications," *IEEE Communications Magazine*, 2015. [Online]. Available: [https://www.ofcom.org.uk/\\_\\_data/assets/pdf\\_file/0023/69422/spectrum\\_above\\_6\\_ghz\\_cfi.pdf](https://www.ofcom.org.uk/__data/assets/pdf_file/0023/69422/spectrum_above_6_ghz_cfi.pdf). [Accessed: 03-Jun-2015].
- [23] Y. Niu, Y. Li, D. Jin, L. Su, and A. V. Vasilakos, "A survey of millimeter wave communications (mmWave) for 5G: opportunities and challenges," *Wirel. Networks*, vol. 21, no. 8, pp. 2657–2676, Nov. 2015.
- [24] J. Zhang, X. Ge, Q. Li, M. Guizani, and Y. Zhang, "5G Millimeter-Wave Antenna Array: Design and Challenges," *IEEE Wirel. Commun.*, vol. 24, no. 2, pp. 106–112, Apr. 2017.
- [25] V. Chandrasekhar, J. G. Andrews, and A. Gatherer, "Femtocell networks: A survey," *IEEE Commun. Mag.*, vol. 46, no. 9, pp. 59–67, Sep. 2008.
- [26] Final Acts WRC, "In World Radiocommunication Conference Geneva: International Telecommunication Union," 2015.
- [27] A. Gupta and R. K. Jha, "A Survey of 5G Network: Architecture and Emerging Technologies," *IEEE Access*, vol. 3, pp. 1206–1232, 2015.
- [28] S. Rajagopal, S. Abu-Surra, Zhouyue Pi, and F. Khan, "Antenna Array Design for Multi-Gbps mmWave Mobile Broadband Communication," in *2011 IEEE Global Telecommunications Conference - GLOBECOM 2011*, 2011, pp. 1–6.
- [29] L. Liao and X. Duan, "Graphene for radio frequency electronics," *Mater. Today*, vol. 15, no. 7–8, pp. 328–338, Jul. 2012.
- [30] X. Li *et al.*, "Large-Area Synthesis of High-Quality and Uniform Graphene Films on Copper Foils," *Science (80-. )*, vol. 324, no. 5932, pp. 1312–1314, Jun. 2009.
- [31] Yi Huang, Lin-Sheng Wu, Min Tang, and Junfa Mao, "Design of a Beam Reconfigurable THz Antenna With Graphene-Based Switchable High-Impedance Surface," *IEEE Trans. Nanotechnol.*, vol. 11, no. 4, pp. 836–842, Jul. 2012.
- [32] Z. Xu, X. Dong, and J. Bornemann, "Design of a Reconfigurable MIMO System for THz Communications Based on Graphene Antennas," *IEEE Trans. Terahertz Sci. Technol.*, vol. 4, no. 5, pp. 609–617, Sep. 2014.
- [33] M. U. Memon and S. Lim, "Frequency-Tunable Compact Antenna Using Quarter-Mode Substrate Integrated Waveguide," *IEEE Antennas Wirel. Propag. Lett.*, vol. 14, no. August 2016, pp. 1606–1609, 2015.

- [34] F. A. Ghaffar and A. Shamim, "A Ferrite LTCC Based Dual Purpose Helical Antenna Providing Bias for Tunability," *IEEE Antennas Wirel. Propag. Lett.*, vol. 14, pp. 831–834, 2015.
- [35] A. C. Polycarpou, M. A. Christou, and N. C. Papanicolaou, "Tunable Patch Antenna Printed on a Biased Nematic Liquid Crystal Cell," *IEEE Trans. Antennas Propag.*, vol. 62, no. 10, pp. 4980–4987, Oct. 2014.
- [36] M. Wang, H. F. Ma, H. C. Zhang, W. X. Tang, X. R. Zhang, and T. J. Cui, "Frequency-Fixed Beam-Scanning Leaky-Wave Antenna Using Electronically Controllable Corrugated Microstrip Line," *IEEE Trans. Antennas Propag.*, vol. 66, no. 9, pp. 4449–4457, Sep. 2018.
- [37] S.-A. Choi, S.-H. Lee, and H.-K. Choi, "Design of the ESPAR antenna with improved DC bias," *Microw. Opt. Technol. Lett.*, vol. 57, no. 10, pp. 2281–2286, Oct. 2015.
- [38] A. Othman, R. Barrak, G. I. Abib, and M. Mabrouk, "A varactor based tunable RF filter for multistandard wireless communication receivers," *AEU - Int. J. Electron. Commun.*, vol. 102, pp. 69–77, Apr. 2019.
- [39] S.-S. Oh, W.-K. Park, Y.-B. Jung, T.-I. Choi, and Y.-H. Lee, "Frequency-tunable open-ring microstrip antenna with optimally-positioned varactors for radiated-power in situ measurements," *AEU - Int. J. Electron. Commun.*, vol. 68, no. 9, pp. 841–845, Sep. 2014.
- [40] A. J. Alazemi, B. Avser, and G. M. Rebeiz, "Low-profile tunable multi-band LTE antennas with series and shunt tuning devices," *AEU - Int. J. Electron. Commun.*, vol. 110, p. 152855, Oct. 2019.
- [41] D. Cure, T. M. Weller, T. Price, F. A. Miranda, and F. W. Van Keuls, "Low-Profile Tunable Dipole Antenna Using Barium Strontium Titanate Varactors," *IEEE Trans. Antennas Propag.*, vol. 62, no. 3, pp. 1185–1193, Mar. 2014.
- [42] E. González-Rodríguez *et al.*, "Tunable ferroelectric impedance matching networks and their impact on digital modulation system performance," *AEU - Int. J. Electron. Commun.*, vol. 67, no. 12, pp. 1107–1117, Dec. 2013.
- [43] I. T. E. Elfergani, R. A. Abd-Alhameed, C. H. See, T. Sadeghpour, J. M. Noras, and S. M. R. Jones, "Small size tuneable printed F-slot antenna for mobile handset applications," *Microw. Opt. Technol. Lett.*, vol. 54, no. 3, pp. 794–802, Mar. 2012.

- [86] A. Mehdipour, I. D. Rosca, A.-R. Sebak, C. W. Trueman, and S. V. Hoa, “Carbon Nanotube Composites for Wideband Millimeter-Wave Antenna Applications,” *IEEE Trans. Antennas Propag.*, vol. 59, no. 10, pp. 3572–3578, Oct. 2011.
- [87] K. S. Novoselov *et al.*, “Electric Field Effect in Atomically Thin Carbon Films,” *Science (80-. )*, vol. 306, no. 5696, pp. 666–669, Oct. 2004.
- [88] T. Palacios, A. Hsu, and H. Wang, “Applications of graphene devices in RF communications,” *IEEE Commun. Mag.*, vol. 48, no. 6, pp. 122–128, Jun. 2010.
- [89] J. S. Bunch, “Mechanical and Electrical Properties of Graphene Sheets,” Cornell University, 2008.
- [90] R. Vajtai, *Springer Handbook of Nanomaterials*. Berlin, Heidelberg: Springer Berlin Heidelberg, 2013.
- [91] S. Gulfam, “Graphene: structure and shape | Graphene-Info,” *JAMIA MEDIA*, 2012. [Online]. Available: <https://jamiamedia.com/2019/08/graphene-structure-and-shape/>. [Accessed: 01-Nov-2019].
- [92] “Graphene,” *TUTORIAL FREE*, 2006. [Online]. Available: <http://www.tutorialgratis.com.br/grafeno-do-brazil/>. [Accessed: 01-Nov-2019].
- [93] V. J. Surya, K. Iyakutti, H. Mizuseki, and Y. Kawazoe, “Tuning Electronic Structure of Graphene: A First-Principles Study,” *IEEE Trans. Nanotechnol.*, vol. 11, no. 3, pp. 534–541, May 2012.
- [94] L. A. Falkovsky, “Optical properties of graphene,” *J. Phys. Conf. Ser.*, vol. 129, p. 012004, Oct. 2008.
- [95] G. W. Hanson, “Dyadic Green’s functions and guided surface waves for a surface conductivity model of graphene,” *J. Appl. Phys.*, vol. 103, no. 6, p. 064302, Mar. 2008.
- [96] MuonRay, “The Spacecraft That Requires no Fuel: Graphene Photoelectric Solar Sails,” 2016. [Online]. Available: <http://muonray.blogspot.com/2016/06/>.
- [97] J.-S. Moon and D. K. Gaskill, “Graphene: Its Fundamentals to Future Applications,” *IEEE Trans. Microw. Theory Tech.*, vol. 59, no. 10, pp. 2702–2708, Oct. 2011.

- [98] G. N. Dash, S. R. Pattanaik, and S. Behera, “Graphene for Electron Devices: The Panorama of a Decade,” *IEEE J. Electron Devices Soc.*, vol. 2, no. 5, pp. 77–104, Sep. 2014.
- [99] L. Pierantoni, D. Mencarelli, M. Bozzi, R. Moro, and S. Bellucci, “Microwave applications of graphene for tunable devices,” in *2014 44th European Microwave Conference*, 2014, pp. 1456–1459.
- [100] A. Reina *et al.*, “Large Area, Few-Layer Graphene Films on Arbitrary Substrates by Chemical Vapor Deposition,” *Nano Lett.*, vol. 9, no. 1, pp. 30–35, Jan. 2009.
- [101] W. Tian, W. Li, W. Yu, and X. Liu, “A Review on Lattice Defects in Graphene: Types, Generation, Effects and Regulation,” *Micromachines*, vol. 8, no. 5, p. 163, May 2017.
- [102] X. Yu, “FDTD Modeling of Graphene-Based RF Devices: Fundamental Aspects and Applications,” University of Toronto, 2013.
- [103] M. Dragoman, M. Aldrigo, A. Dinescu, D. Dragoman, and A. Costanzo, “Towards a terahertz direct receiver based on graphene up to 10 THz,” *J. Appl. Phys.*, vol. 115, no. 4, p. 044307, Jan. 2014.
- [104] M. Aldrigo, M. Dragoman, A. Constanzo, and D. Dragoman, “Graphene as a high impedance surface for ultra-wideband electromagnetic waves,” *J. Appl. Phys.*, vol. 114, no. 18, pp. 36–41, 2013.
- [105] P.-Y. Chen, C. Argyropoulos, and A. Alu, “Terahertz Antenna Phase Shifters Using Integrally-Gated Graphene Transmission-Lines,” *IEEE Trans. Antennas Propag.*, vol. 61, no. 4, pp. 1528–1537, Apr. 2013.
- [106] S. E. Hosseinijad and N. Komjani, “Waveguide-Fed Tunable Terahertz Antenna Based on Hybrid Graphene-Metal Structure,” *IEEE Trans. Antennas Propag.*, vol. 64, no. 9, pp. 3787–3793, Sep. 2016.
- [107] D. Correas-Serrano, J. S. Gomez-Diaz, J. Perruisseau-Carrier, and A. Alvarez-Melcon, “Graphene-Based Plasmonic Tunable Low-Pass Filters in the Terahertz Band,” *IEEE Trans. Nanotechnol.*, vol. 13, no. 6, pp. 1145–1153, Nov. 2014.
- [108] P. Russer, N. Fichtner, P. Lugli, W. Porod, J. A. Russer, and H. Yordanov, “Nanoelectronics-Based Integrate Antennas,” *IEEE Microw. Mag.*, vol. 11, no. 7, pp. 58–71, Dec. 2010.

- [109] A. Scidà *et al.*, “Application of graphene-based flexible antennas in consumer electronic devices,” *Mater. Today*, vol. 21, no. 3, pp. 223–230, Apr. 2018.
- [110] G. Deligeorgis *et al.*, “Microwave propagation in graphene,” *Appl. Phys. Lett.*, vol. 95, no. 7, pp. 1–8, 2009.
- [111] D. Neculoiu *et al.*, “Electromagnetic propagation in graphene in the mm-wave frequency range,” *Eur. Microw. Week 2010, EuMW2010 Connect. World, Conf. Proc. - Eur. Microw. Conf. EuMC 2010*, no. September, pp. 1619–1622, 2010.
- [112] M. Yasir *et al.*, “Integration of Antenna Array and Self-Switching Graphene Diode for Detection at 28 GHz,” *IEEE Electron Device Lett.*, vol. 40, no. 4, pp. 628–631, Apr. 2019.
- [113] H. Giddens, L. Yang, J. Tian, and Y. Hao, “Mid-Infrared Reflect-Array Antenna With Beam Switching Enabled by Continuous Graphene Layer,” *IEEE Photonics Technol. Lett.*, vol. 30, no. 8, pp. 748–751, Apr. 2018.
- [114] W. Fuscaldo, P. Burghignoli, P. Baccarelli, and A. Galli, “A Reconfigurable Substrate–Superstrate Graphene-Based Leaky-Wave THz Antenna,” *IEEE Antennas Wirel. Propag. Lett.*, vol. 15, pp. 1545–1548, 2016.
- [115] D. Correas-Serrano, J. S. Gomez-Diaz, A. Alu, and A. Alvarez-Melcon, “Electrically and Magnetically Biased Graphene-Based Cylindrical Waveguides: Analysis and Applications as Reconfigurable Antennas,” *IEEE Trans. Terahertz Sci. Technol.*, vol. 5, no. 6, pp. 951–960, Nov. 2015.
- [116] Y. Wu, J. Yu, S.-W. Qu, Y. Yao, X. Cheng, and X. Chen, “Circular beam-reconfigurable antenna base on graphene-metal hybrid,” *Electron. Lett.*, vol. 52, no. 7, pp. 494–496, Apr. 2016.
- [117] Y. Dong, P. Liu, D. Yu, G. Li, and F. Tao, “Dual-Band Reconfigurable Terahertz Patch Antenna With Graphene-Stack-Based Backing Cavity,” *IEEE Antennas Wirel. Propag. Lett.*, vol. 15, pp. 1541–1544, 2016.
- [118] E. Carrasco and J. Perruisseau-Carrier, “Reflectarray Antenna at Terahertz Using Graphene,” *IEEE Antennas Wirel. Propag. Lett.*, vol. 12, pp. 253–256, 2013.
- [119] Z. Chang, B. You, L.-S. Wu, M. Tang, Y.-P. Zhang, and J.-F. Mao, “A Reconfigurable Graphene Reflectarray for Generation of Vortex THz Waves,” *IEEE Antennas Wirel. Propag. Lett.*, vol. 15, pp. 1537–1540, 2016.

- [120] M. Esquius-Morote, J. S. Gomez-Diaz, and J. Perruisseau-Carrier, “Sinusoidally Modulated Graphene Leaky-Wave Antenna for Electronic Beamscanning at THz,” *IEEE Trans. Terahertz Sci. Technol.*, vol. 4, no. 1, pp. 116–122, Jan. 2014.
- [121] F. Liang, Z.-Z. Yang, Y.-X. Xie, H. Li, D. Zhao, and B.-Z. Wang, “Beam-Scanning Microstrip Quasi-Yagi–Uda Antenna Based on Hybrid Metal-Graphene Materials,” *IEEE Photonics Technol. Lett.*, vol. 30, no. 12, pp. 1127–1130, Jun. 2018.
- [122] T. Leng, X. Huang, K. Chang, J. Chen, M. A. Abdalla, and Z. Hu, “Graphene Nanoflakes Printed Flexible Meandered-Line Dipole Antenna on Paper Substrate for Low-Cost RFID and Sensing Applications,” *IEEE Antennas Wirel. Propag. Lett.*, vol. 15, no. c, pp. 1565–1568, 2016.
- [123] M. Akbari, M. W. A. Khan, M. Hasani, T. Bjorninen, L. Sydanheimo, and L. Ukkonen, “Fabrication and Characterization of Graphene Antenna for Low-Cost and Environmentally Friendly RFID Tags,” *IEEE Antennas Wirel. Propag. Lett.*, vol. 15, no. c, pp. 1569–1572, 2016.
- [124] K. Arapov *et al.*, “Graphene screen-printed radio-frequency identification devices on flexible substrates,” *Phys. status solidi - Rapid Res. Lett.*, vol. 10, no. 11, pp. 812–818, Nov. 2016.
- [125] K. N. Parrish, “Nanoscale Graphene for Rf Circuits and Systems,” The University of Texas at Austin, 2013.
- [126] A. Lamminen *et al.*, “Graphene-Flakes Printed Wideband Elliptical Dipole Antenna for Low-Cost Wireless Communications Applications,” *IEEE Antennas Wirel. Propag. Lett.*, vol. 16, pp. 1883–1886, 2017.
- [127] A. Katsounaros, M. T. Cole, H. M. Tuncer, W. I. Milne, and Y. Hao, “Near-field characterization of chemical vapor deposition graphene in the microwave regime,” *Appl. Phys. Lett.*, vol. 102, no. 23, p. 233104, Jun. 2013.
- [128] X. Huang *et al.*, “Highly Flexible and Conductive Printed Graphene for Wireless Wearable Communications Applications,” *Sci. Rep.*, vol. 5, no. 1, p. 18298, Nov. 2016.
- [129] H.-J. Lee, E. Kim, J.-G. Yook, and J. Jung, “Intrinsic characteristics of transmission line of graphenes at microwave frequencies,” *Appl. Phys. Lett.*, vol. 100, no. 22, p. 223102, May 2012.

- [130] Z. Hu, M. Aqeeli, X. Zhang, X. Huang, and A. Alburaikan, "Design of broadband and tunable terahertz absorbers based on graphene metasurface: equivalent circuit model approach," *IET Microwaves, Antennas Propag.*, vol. 9, no. 4, pp. 307–312, Mar. 2015.
- [131] Bingzheng Xu, Changqing Gu, Zhuo Li, Liangliang Liu, and Zhenyi Niu, "A Novel Absorber With Tunable Bandwidth Based on Graphene," *IEEE Antennas Wirel. Propag. Lett.*, vol. 13, pp. 822–825, 2014.
- [132] M. Olszewska-Placha, B. Salski, D. Janczak, P. R. Bajurko, W. Gwarek, and M. Jakubowska, "A Broadband Absorber With a Resistive Pattern Made of Ink With Graphene Nano-Platelets," *IEEE Trans. Antennas Propag.*, vol. 63, no. 2, pp. 565–572, Feb. 2015.
- [133] A. G. D'Aloia, M. D'Amore, and M. S. Sarto, "Adaptive Broadband Radar Absorber Based on Tunable Graphene," *IEEE Trans. Antennas Propag.*, vol. 64, no. 6, pp. 2527–2531, Jun. 2016.
- [134] M. Biabanifard and M. S. Abrishamian, "Multi-band circuit model of tunable THz absorber based on graphene sheet and ribbons," *AEU - Int. J. Electron. Commun.*, vol. 95, pp. 256–263, Oct. 2018.
- [135] S. Bellucci, M. Bozzi, A. Cataldo, R. Moro, D. Mencarelli, and L. Pierantoni, "Graphene as a tunable resistor," in *2014 International Semiconductor Conference (CAS)*, 2014, pp. 17–20.
- [136] K. Na, H. Ma, J. Park, J. Yeo, J.-U. Park, and F. Bien, "Graphene-Based Wireless Environmental Gas Sensor on PET Substrate," *IEEE Sens. J.*, vol. 16, no. 12, pp. 5003–5009, Jun. 2016.
- [137] D. Tang *et al.*, "Highly sensitive wearable sensor based on a flexible multi-layer graphene film antenna," *Sci. Bull.*, vol. 63, no. 9, pp. 574–579, May 2018.
- [138] X. He, "Tunable terahertz graphene metamaterials," *Carbon N. Y.*, vol. 82, no. C, pp. 229–237, Feb. 2015.
- [139] K.-Y. Shin, M. Kim, J. S. Lee, and J. Jang, "Highly Omnidirectional and Frequency Controllable Carbon/Polyaniline-based 2D and 3D Monopole Antenna," *Sci. Rep.*, vol. 5, no. 1, p. 13615, Nov. 2015.
- [140] C. Fan, B. Wu, R. Song, Y. Zhao, Y. Zhang, and D. He, "Electromagnetic shielding and multi-beam radiation with high conductivity multilayer graphene film," *Carbon N. Y.*, vol. 155, pp. 506–513, Dec. 2019.

- [141] A.-C. Bunea, D. Neculoiu, M. Dragoman, G. Konstantinidis, and G. Deligeorgis, “X band tunable slot antenna with graphene patch,” in *2015 European Microwave Conference (EuMC)*, 2015, no. 318352, pp. 614–617.
- [142] M. Yasir *et al.*, “A Planar Antenna With Voltage-Controlled Frequency Tuning Based on Few-Layer Graphene,” *IEEE Antennas Wirel. Propag. Lett.*, vol. 16, pp. 2380–2383, 2017.
- [143] M. Cao, R. Qin, C. Qiu, and J. Zhu, “Matching design and mismatching analysis towards radar absorbing coatings based on conducting plate,” *Mater. Des.*, vol. 24, no. 5, pp. 391–396, 2003.
- [144] S. Cao, H. Liu, L. Yang, Y. Zou, X. Xia, and H. Chen, “The effect of microstructure of graphene foam on microwave absorption properties,” *J. Magn. Magn. Mater.*, vol. 458, pp. 217–224, Jul. 2018.
- [145] S. Ramo, J. R. Whinnery, and T. Van Duzar, *Fields and Waves in Communication Electronics*. New York: J. Wiley., 1997.
- [146] H. Liu, W. Yang, F. He, Y. Li, X. Yang, and K. Zhang, “Graphene-based composite with microwave absorption property prepared by in situ reduction,” *Polym. Compos.*, vol. 35, no. 3, pp. 461–467, Mar. 2014.
- [147] C.-Y. Chen *et al.*, “Remarkable microwave absorption performance of graphene at a very low loading ratio,” *Compos. Part B Eng.*, vol. 114, pp. 395–403, Apr. 2017.
- [148] J. Syurik, O. A. Ageev, D. I. Cherednichenko, B. G. Konoplev, and A. Alexeev, “Non-linear conductivity dependence on temperature in graphene-based polymer nanocomposite,” *Carbon N. Y.*, vol. 63, pp. 317–323, Nov. 2013.
- [149] N. Song, C. Lu, C. Chen, C. Ma, and Q. Kong, “Effect of annealing temperature on the mechanical properties of flexible graphene films,” *New Carbon Mater.*, vol. 32, no. 3, pp. 221–226, Jun. 2017.
- [150] S. Ma *et al.*, “Effects of temperature on microstructure and mechanical properties of IN718 reinforced by reduced graphene oxide through spark plasma sintering,” *J. Alloys Compd.*, vol. 767, pp. 675–681, Oct. 2018.
- [151] L. L. Dong *et al.*, “Sintering effect on microstructural evolution and mechanical properties of spark plasma sintered Ti matrix composites reinforced by reduced graphene oxides,” *Ceram. Int.*, vol. 44, no. 15, pp. 17835–17844, Oct. 2018.



- [152] T. C. Li, C. F. Han, K. C. Hsieh, and J. F. Lin, “Effects of thin titanium and graphene depositions and annealing temperature on electrical, optical, and mechanical properties of IGZO/Ti/graphene/PI specimen,” *Ceram. Int.*, vol. 44, no. 6, pp. 6573–6583, 2018.
- [153] J. S. Im, S. J. Kim, P. H. Kang, and Y.-S. Lee, “The improved electrical conductivity of carbon nanofibers by fluorinated MWCNTs,” *J. Ind. Eng. Chem.*, vol. 15, no. 5, pp. 699–702, Sep. 2009.
- [154] J. S. Im, J. G. Kim, and Y.-S. Lee, “Fluorination effects of carbon black additives for electrical properties and EMI shielding efficiency by improved dispersion and adhesion,” *Carbon N. Y.*, vol. 47, no. 11, pp. 2640–2647, Sep. 2009.
- [155] H. Pang, C. Chen, Y.-C. Zhang, P.-G. Ren, D.-X. Yan, and Z.-M. Li, “The effect of electric field, annealing temperature and filler loading on the percolation threshold of polystyrene containing carbon nanotubes and graphene nanosheets,” *Carbon N. Y.*, vol. 49, no. 6, pp. 1980–1988, May 2011.
- [156] Graphene Supermarket, “Conductive Graphene Sheets, 8"x4"." [Online]. Available: <https://graphene-supermarket.com/Conductive-Graphene-Sheets.html>. [Accessed: 13-Dec-2019].
- [157] RS Online, “Kapton HN Thermal Insulating Film, 304mm x 200mm x 0.075mm,” 2018. [Online]. Available: <https://my.rs-online.com/web/p/thermal-insulating-films/5363968/>. [Accessed: 03-Sep-2019].
- [158] C. P. Wen, “Coplanar Waveguide: A Surface Strip Transmission Line Suitable for Nonreciprocal Gyromagnetic Device Applications,” *IEEE Trans. Microw. Theory Tech.*, vol. 17, no. 12, pp. 1087–1090, Dec. 1969.
- [159] F. M. Tanyer- Tigrek, I. E. Lager, and L. P. Ligthart, “A CPW-Fed Printed Loop Antenna for Ultra-Wideband Applications, and its Linear-Array Performance,” *IEEE Antennas Propag. Mag.*, vol. 52, no. 4, pp. 31–40, Aug. 2010.
- [160] S. Ahmed, F. A. Tahir, A. Shamim, and H. M. Cheema, “A Compact Kapton-Based Inkjet-Printed Multiband Antenna for Flexible Wireless Devices,” *IEEE Antennas Wirel. Propag. Lett.*, vol. 14, pp. 1802–1805, 2015.
- [161] R. N. Simons, *Coplanar Waveguide Circuits, Components, and Systems*, vol. 7. New York, USA: John Wiley & Sons, Inc., 2001.

- [162] Taeksoo Ji, H. Yoon, J. K. Abraham, and V. K. Varadan, “Ku-band antenna array feed distribution network with ferroelectric phase shifters on silicon,” *IEEE Trans. Microw. Theory Tech.*, vol. 54, no. 3, pp. 1131–1138, Mar. 2006.
- [163] X. Huang *et al.*, “Binder-free highly conductive graphene laminate for low cost printed radio frequency applications,” *Appl. Phys. Lett.*, vol. 106, no. 20, p. 203105, May 2015.
- [164] “Field-Emission Scanning Electron Microscope (FESEM).” [Online]. Available: <http://mjiit.utm.my/microscopy-lab/field-emission-scanning-electron-microscope-fesem/>. [Accessed: 10-Oct-2019].
- [165] “alpha300 R – Confocal Raman Imaging.” [Online]. Available: <https://www.witec.de/techniques/raman/>. [Accessed: 16-Nov-2019].
- [166] B. Fan, Y. Liu, D. He, and J. Bai, “Influences of graphene nanoplatelet aspect ratio and thermal treatment on dielectric performances of poly(methyl methacrylate) composites,” *High Volt.*, vol. 1, no. 4, pp. 146–150, Dec. 2016.
- [167] A. Vijayaraghavan, “Graphene – Properties and Characterization,” in *Springer Handbook of Nanomaterials*, R. Vajtai, Ed. Berlin, Heidelberg: Springer Berlin Heidelberg, 2013, pp. 39–82.
- [168] R. U. Rehman Sagar *et al.*, “Defect-induced, temperature-independent, tunable magnetoresistance of partially fluorinated graphene foam,” *Carbon N. Y.*, 2018.

## LIST OF PUBLICATIONS

S. N. H. Sa'don, M. R. Kamarudin, F. Ahmad, M. Jusoh, and H. A. Majid, "Graphene array antenna for 5G applications," *Appl. Phys. A Mater. Sci. Process.*, vol. 123, no. 2, pp. 1–4, 2017.

S. N. H. Sa'don, M. H. Jamaluddin, M. R. Kamarudin, F. Ahmad, and S. H. Dahlan, "A 5G graphene antenna produced by screen printing method," *Indones. J. Electr. Eng. Comput. Sci.*, vol. 15, no. 2, pp. 950–055, 2019.

S. N. H. Sa'don, M. H. Jamaluddin, M. R. Kamarudin, and F. Ahmad, "Graphene Based Antenna Array for 5G Applications," in *2018 IEEE International RF and Microwave Conference (RFM)*, 2019, pp. 65–68.

S. N. H. Sa'don et al., "Analysis of Graphene Antenna Properties for 5G Applications," *Sensors*, vol. 19, no. 22, p. 4835, Nov. 2019.

S. N. H. Sa'don et al., "Characterisation of tunable graphene antenna," *AEU - Int. J. Electron. Commun.*, vol. 118, p. 153170, May 2020.